



Whole-tumor ADC histogram analysis for differentiating endometriosis-related tumors: seromucinous borderline tumor, clear cell carcinoma and endometrioid carcinoma

Jing Lu¹ · Shuhui Zhao^{1,2} · Fenghua Ma^{1,3} · Haiming Li^{1,4} · Yong'ai Li¹ · Jinwei Qiang¹

Received: 26 September 2022 / Revised: 3 November 2022 / Accepted: 4 November 2022 / Published online: 19 November 2022
© The Author(s), under exclusive licence to Springer Science+Business Media, LLC, part of Springer Nature 2022

Abstract

Purpose To investigate the feasibility of whole-tumor apparent diffusion coefficient (ADC) histogram analysis for improving the differentiation of endometriosis-related tumors: seromucinous borderline tumor (SMBT), clear cell carcinoma (CCC) and endometrioid carcinoma (EC).

Methods Clinical features, solid component ADC (ADC_{SC}) and whole-tumor ADC histogram-derived parameters (volume, the ADC_{mean} , 10th, 50th and 90th percentile ADCs, inhomogeneity, skewness, kurtosis and entropy) were compared among 22 SMBTs, 42 CCCs and 21 ECs. Statistical analyses were performed using chi-square test, one-way ANOVA or Kruskal–Wallis test, and receiver operating characteristic curves.

Results A significantly higher ADC_{SC} and smaller volume were associated with SMBT than with CCC/EC. The ADC_{mean} was significantly higher in CCC than in EC. The 10th percentile ADC was significantly lower in EC than in SMBT/CCC. The 50th and 90th percentile ADCs were significantly higher in CCC than in SMBT/EC. For differentiating SMBT from CCC, AUCs of the ADC_{SC} , volume, and 50th and 90th percentile ADCs were 0.97, 0.86, 0.72 and 0.81, respectively. For differentiating SMBT from EC, AUCs of the ADC_{SC} , volume and 10th percentile ADC were 0.97, 0.71 and 0.72, respectively. For differentiating CCC from EC, AUCs of the ADC_{mean} and 10th, 50th and 90th percentile ADCs were 0.79, 0.72, 0.81 and 0.85, respectively.

Conclusion Whole-tumor ADC histogram analysis was valuable for differentiating endometriosis-related tumors, and the 90th percentile ADC was optimal in differentiating CCC from EC.

✉ Yong'ai Li
pingyaoai@163.com

✉ Jinwei Qiang
dr.jinweiqiang@163.com

Jing Lu
wohelujing@sohu.com

Shuhui Zhao
zhaoshuhui1029@163.com

Fenghua Ma
mafenghua9602@163.com

Haiming Li
lihaiming0109@163.com

¹ Department of Radiology, Jinshan Hospital, Fudan University, 1508 Longhang Road, Shanghai 201508, People's Republic of China

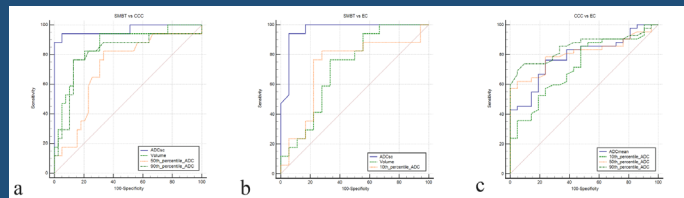
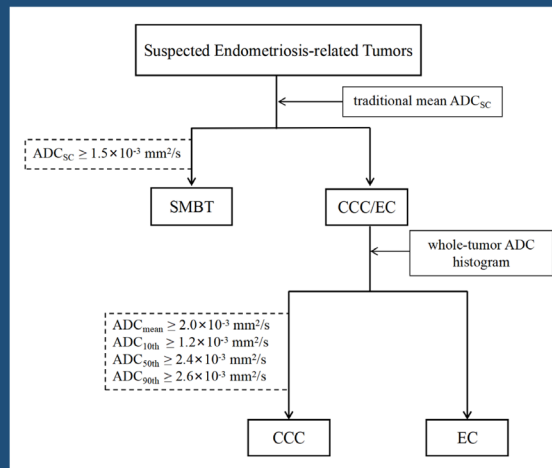
² Department of Radiology, Xinhua Hospital, Medical College of Shanghai Jiao Tong University, Shanghai 200092, People's Republic of China

³ Department of Radiology, Obstetrics and Gynecology Hospital, Fudan University, 419 Fangxie Road, Shanghai 200011, People's Republic of China

⁴ Department of Radiology, Shanghai Cancer Center, Fudan University, 270 Dongan Road, Shanghai 200032, People's Republic of China

Graphical abstract

Whole-tumor ADC histogram analysis for differentiating endometriosis-related tumors: SMBT, CCC and EC



Whole-tumor ADC histogram analysis had both complementary role in differentiate SMBT from CCC/EC, and unique advantages in differentiating CCC from EC.

Abdominal Radiology
The Official Journal of the Society of Abdominal Radiology www.abdominalradiology.org

Jing Lu et al; 2022

Keywords Seromucinous borderline tumor · Clear cell carcinoma · Endometrioid carcinoma · Magnetic resonance imaging · Apparent diffusion coefficient · Histogram analysis

Introduction

Endometriosis-related ovarian neoplasms are now attracting attention because they show common molecular genetic changes [1, 2]. Endometriosis is a common disease involving approximately 5–15% of women of reproductive age [3]. It occurs most frequently in ovary, with 1–2% endometriosis can transform into endometriosis-associated ovarian cancer [3]. It is reported that approximately 30–35% of clear cell carcinomas (CCCs), 23–42% of endometrioid carcinomas (ECs) and 30–50% seromucinous borderline tumors (SMBTs) are associated with endometriosis [2, 4]. SMBTs are the most common subtype of seromucinous tumors of the ovary which were formerly classified as the Mullerian or endocervical subtype of mucinous tumors. Up to 90% of SMBT patients present as International Federation of Gynecology and Obstetrics (FIGO) stage I, with an excellent prognosis even for advanced-stage disease [5]. While CCCs and ECs are associated with a poorer prognosis. According to the National Comprehensive Cancer Network (NCCN) guidelines, patients with early-stage ECs and stage I-III borderline tumors are candidates for fertility-sparing surgery which may be performed laparoscopically [7]. However,

fertility preservation is not recommended for any stage of CCCs as well as high-grade serous cancers [7]. Surgery for patients with CCC should be performed by open laparotomy [7]. Although intraoperative histologic evaluation with frozen sections was performed to guide gynecologists for the most appropriate surgical procedure [7, 8], huge size and diversity and heterogeneity of ovarian tumors compromise the accuracy of frozen section diagnosis, with 81% for early-stage malignant tumors and only 60–75% for borderline tumors [8]. Histologically, CCC potentially overlap with EC, borderline tumors as well as metastatic carcinoma, particularly in small biopsy specimens or during intra-operative assessment [7–9]. Therefore, it is clinically important to pre-operatively differentiate among SMBT, CCC and EC for an optimal surgical planning [1, 10].

Studies have shown that the magnetic resonance imaging (MRI) findings of SMBT, CCC and EC often overlap and frequently appear as large cystic masses with hyperintensity on T1- and T2-weighted imaging (T1/T2WI) and intracystic vascularized mural nodules and/or solid components [1, 11–13]. Morphological differentiation of CCC and EC achieves only a moderate diagnostic accuracy [10, 14]. Though the mean apparent diffusion coefficient of the solid

components (ADC_{SC}) is a useful parameter for differentiating SMBT from CCC and EC, it is inefficient for differentiating CCC from EC [1, 15]. In addition, the traditional mean ADC_{SC} takes no account of heterogeneity within an entire tumor. Therefore, a more effective method is warranted to investigate the differentiation of SMBT, CCC and EC.

Histogram analysis of the ADC can interrogate the biological heterogeneity of tumors by classifying domains of different diffusion [16]. Recently, solid-tumor histogram analysis of the ADC has been used for the differential diagnosis and prediction of chemotherapy response in epithelial ovarian tumors [16–18]; whole-tumor histogram analysis of the ADC has also been studied in diagnostic, grading, prognostic and predictive applications in many tumors including ovarian cancers [19–23]. Therefore, this study aimed to investigate the feasibility of histogram analysis of the whole-tumor ADC in the differentiation of SMBT, CCC and EC by comparing with the traditional ADC_{SC} .

Material and methods

Study population

This retrospective study was approved by the institutional review board, and the requirement for informed consent was waived for all patients. Between February 2011 and April 2021, patients with SMBT, CCC and EC proven by histology were reviewed. The inclusion criteria were as follows: (1) patients undergoing abdominopelvic MRI before treatment and the interval less than 2 weeks; (2) MRI including diffusion-weighted imaging (DWI) with b factors of 0 and 1000 s/mm^2 ; and (3) tumors removed by surgery and proven by histopathology to be endometriosis-associated. The exclusion criteria were as follows: (1) tumors without a histopathological confirmation of endometriosis; (2) patients with a tumor too small to be detected on MRI; and (3) MRI scans with poor image quality. Patients' clinical data, including age, laterality, and FIGO stage, were recorded.

MRI technique

MRI was performed with a 1.5-T scanner (Avanto, Siemens, Erlangen, Germany) with a phased array coil. The patients lay in the supine position and breathed freely during acquisition. The scanning range was from the inferior pubic symphysis to the renal hilum and extended beyond the dome of the tumor in cases of large masses. The scanning sequences and parameters are listed in Table 1. Axial DWI was performed using a single-shot echo planar imaging sequence with the diffusion gradient b factors of 0 and 1000 s/mm^2 . Axial and sagittal contrast-enhanced imaging were performed after administering gadolinium chelate (Gd-DTPA, Magnevist;

Table 1 MRI sequences and parameters in patients with SMBT, CCC and EC

Parameters	T1WI	T2WI	T1WI-FS	DWI
Repetition time (ms)	340	8000	196	3200
Echo time (ms)	10	83	2.9	87
Section thickness (mm)	5	5	5	5
Intersection gap (mm)	1.5	1.5	1.5	1.5
Field of view (mm)	238×280	238×280	238×280	238×280
Matrix	256×256	256×256	256×256	128×128
Acquisition time (s)	120	175	40	166
b factors (s/mm^2)	–	–	–	0, 1000

SMBT seromucinous borderline tumor; *CCC* clear cell carcinoma; *EC* endometrioid carcinoma; *MRI* magnetic resonance imaging; *T1WI* T1-weighted imaging; *T2WI* T2-weighted imaging; *FS* fat saturation; *DWI* diffusion-weighted imaging

Bayer Schering, Berlin, Germany) at a dose of 0.2 mL/kg body weight.

Imaging analysis

MR images were independently analyzed by two radiologists (radiologists 1 and 2, with 6 and 11 years of experience in gynecological imaging, respectively) who were blinded to the histopathology. Images were analyzed again by radiologist 1 after an interval of one month. The ADC_{SC} value was measured with an elliptical region of interest (ROI) drawn as large as possible at the solid component on the slice with largest solid component of ADC map, carefully avoiding areas of hemorrhage, necrosis and major vascular structures. Whole-tumor histogram analysis was performed on the ADC map using Fire Voxel (CAI2R, New York University, NY, USA) according to the methods described in a previous study [11]. The ROI was manually delineated slice-by-slice along the contour of the tumor, referring to T2WI (Fig. 1). Then, the volume of interest of the ADC was postprocessed automatically for histogram analysis. The ADC value for each pixel was recorded. An ADC histogram was generated in which the contribution of each individual tumor was weighted according to its volume, with a bin width of $1 \times 10^{-5} mm^2/s$. Histogram-derived parameters, such as volume, the ADC_{mean} , 10th, 50th and 90th percentiles, skewness, kurtosis, inhomogeneity and entropy, were calculated using SPSS software (version 23.0, SPSS, Chicago, IL, USA).

Statistical analysis

Statistical analyses were performed with SPSS software. The normality of variables was tested using the Shapiro–Wilk test. Continuous variables with a normal distribution were presented as the mean \pm standard deviation, while those with

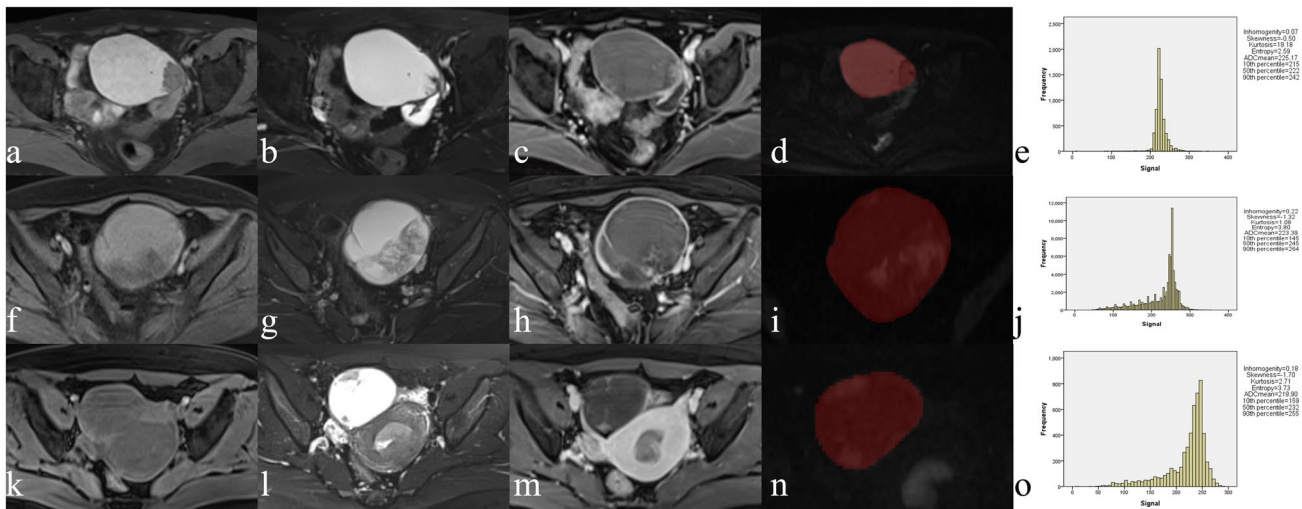


Fig. 1 Whole-tumor ADC histogram analysis in patients with SMBT (a–e), CCC (f–j) and EC (k–o). Referring to T1WI (a, f, k), T2WI (b, g, l) and gadolinium-enhanced T1WI (c, h, m), the ROIs of the whole ovarian tumor were delineated slice-by-slice along the contour of the tumor manually on the ADC map ($b=1000 \text{ s/mm}^2$) (d, i, n), and the histograms of gray-level distribution were calculated with the

parameters listed in the figures (e, j, o). The x-axis and y-axis in the histogram represent the voxel gray-level intensity and frequency of occurrence, respectively. *ADC* apparent diffusion coefficient; *SMBT* seromucinous borderline tumor; *CCC* clear cell carcinoma; *EC* endometrioid carcinoma; *T1WI* T1-weighted imaging; *T2WI* T2-weighted imaging; *ROI* region of interest

a nonnormal distribution were reported as the median (interquartile range). The intra- and interclass correlation coefficients (ICCs) were calculated to evaluate intra- and interobserver agreements, respectively (ICC: 0.00–0.20, poor correlation; 0.21–0.40, fair; 0.41–0.60, moderate; 0.61–0.80, good; and 0.81–1.00, excellent). Categorical variables, including laterality and FIGO stage, were compared using the chi-square test. One-way ANOVA or the Kruskal–Wallis test was performed to compare the differences in age, ADC_{SC} and histogram-derived parameters. Receiver operating characteristic (ROC) curve analysis (MedCalc Software, Mariakerke, Belgium) was used to assess the diagnostic performance and determine optimal cutoff values of the histogram-derived parameters for the differentiation of SMBT, CCC and EC. The Delong test was used to compare the area under the curve (AUC) differences. A p value less than 0.05 was regarded as statistically significant.

Results

Patient demographics

A total of 85 patients (22 with SMBT, 42 with CCC and 21 with EC) were enrolled. The median time interval between the MRI scan and surgery was 5 days. The clinical features of patients are summarized in Table 2. There were significant differences in age among the three groups of patients ($p < 0.001$). Patients with SMBT were significantly younger (39.91 ± 12.08 years) than patients with

CCC (51.48 ± 9.52 years) and EC (52.24 ± 8.15 years) (both $p < 0.001$). There was no significant age difference between patients with CCC and those with EC ($p = 1.000$). Most patients with SMBT, CCC and EC were at an early-stage (stages I and II), and all the patients had a unilateral tumor. No significant differences were observed in the FIGO stage or laterality among the three groups ($p = 0.312$ and 0.722 , respectively).

ADC_{SC} and whole-tumor ADC histogram parameters

The intra- and interobserver agreements were excellent for the ADC_{SC} and histogram parameters, with ICCs of 0.961 (95% confidence interval (CI), 0.941, 0.974) and 0.980 (95% CI, 0.970, 0.987), respectively. The results of the first measurement by radiologist 1 were used for further analyses.

There were significant differences in the ADC_{SC} and whole-tumor histogram parameters, including the volume, ADC_{mean} , and 10th, 50th and 90th percentile ADCs, among the three kinds of tumors (all $p < 0.01$) (Table 3). The ADC_{SC} was significantly higher in SMBT than in CCC and EC (both $p < 0.001$) but was not significantly different between CCC and EC ($p = 0.328$). The volume was significantly smaller in SMBT than in CCC ($p < 0.001$) and EC ($p = 0.024$) but was not significantly different between CCC and EC ($p = 0.559$). The ADC_{mean} was significantly higher in CCC than in EC ($p < 0.001$) but was not significantly different between SMBT and CCC/EC ($p = 0.050$ and 0.418 , respectively). The 10th percentile ADC was significantly lower in EC than in SMBT ($p = 0.033$) and CCC ($p = 0.011$)

Table 2 Clinical features of patients with SMBT, CCC and EC

Features	SMBT (<i>n</i> =22)	CCC (<i>n</i> =42)	EC (<i>n</i> =21)	<i>p</i> value
Age (mean, y)	39.91 ± 12.08 ^{d,e}	51.48 ± 9.52 ^d	52.24 ± 8.15 ^e	< 0.001 ^a
Laterality				0.722 ^b
Right	14	23	11	
Left	8	19	10	
FIGO stage				0.312 ^c
I	18	41	16	
II	2	0	5	
III	2	1	0	
IV	0	0	0	

FIGO international federation of gynecology and obstetrics

^aOne-way ANOVA

^bChi-square test

^cFisher's precision probability test (FIGO I + II vs III + IV)

^{d, e} There was significant difference between the two groups

A significant *p* value was presented as bold

Table 3 ADC of solid components and whole-tumor ADC histogram parameters in SMBT, CCC and EC

Parameters	SMBT (<i>n</i> =22)	CCC (<i>n</i> =42)	EC (<i>n</i> =21)	<i>p</i> value			
				Among all groups	SMBT vs CCC	SMBT vs EC	CCC vs EC
ADC _{sc} *	1.8 (1.7, 1.9)	1.2 (1.0, 1.4)	1.0 (1.0, 1.2)	< 0.001	< 0.001	< 0.001	0.328
Whole-tumor ADC histogram parameters							
Volume (cm ³)	187.6 (76.0, 249.9)	537.0 (338.9, 822.0)	280.1 (140.3, 1022.2)	< 0.001	< 0.001	0.024	0.559
ADC _{mean} *	2.0 ± 0.4	2.2 ± 0.3	1.9 ± 0.3	< 0.001	0.050	0.418	< 0.001
10th percentile ADC*	1.8 (1.5, 2.0)	1.7 (1.3, 2.2)	1.2 (1.0, 1.5) [£]	0.008	1.000	0.033	0.011
50th percentile ADC*	2.1 (1.7, 2.3)	2.5 (2.2, 2.6)	1.9 (1.6, 2.2)	< 0.001	0.015	0.814	< 0.001
90th percentile ADC*	2.4 (2.0, 2.6)	2.7 (2.5, 2.8)	2.4 (2.1, 2.6)	< 0.001	< 0.001	1.000	< 0.001
Skewness	- 0.5 ± 1.4	- 1.2 ± 1.2	- 0.7 ± 1.0	0.055	-	-	-
Kurtosis	3.1 (2.4, 6.2)	2.6 (-0.5, 7.6)	1.4 (-0.9, 4.8)	0.104	-	-	-
Inhomogeneity	0.1 (0.1, 0.1)	0.2 (0.1, 0.2)	0.1 (0.1, 0.2)	0.052	-	-	-
Entropy	3.5 ± 0.4	3.6 ± 0.5	3.8 ± 0.5	0.115	-	-	-

ADC apparent diffusion coefficient; ADC_{sc} solid component ADC; *p* value, One-way ANOVA or Kruskal–Wallis

A significant *p* value was presented as bold

* × 10⁻³ mm²/s

but was not significantly different between SMBT and CCC (*p* = 1.000). The 50th and 90th percentile ADCs were significantly higher in CCC than in SMBT and EC (*p* = 0.015, *p* < 0.001 and both *p* < 0.001, respectively) but were not significantly different between SMBT and EC (*p* = 0.814 and 1.000, respectively). There were no significant differences found in other histogram-derived parameters, including skewness, kurtosis, inhomogeneity or entropy, among the three tumors.

For differentiating SMBT from CCC, the AUCs of the ADC_{sc}, volume, and 50th and 90th percentile ADCs were 0.97, 0.86, 0.72 and 0.81, respectively, with a significant difference between the ADC_{sc} and 50th percentile ADC (*p* = 0.003) (Table 4, Fig. 2) and no significant differences between the ADC_{sc} and volume or 90th percentile ADC (*p* = 0.097 and 0.053, respectively). For differentiating SMBT from EC, the ADC_{sc} had a significantly larger AUC than the volume and 10th percentile ADC (0.97 vs

Table 4 Diagnostic performance of ADC of solid components and whole-tumor histogram parameters in differentiating SMBT, CCC and EC

Parameters	SMBT vs CCC			SMBT vs EC			CCC vs EC					
	AUC	Sensitivity (%)	Specificity (%)	Cutoff value	AUC	Sensitivity (%)	Specificity (%)	Cutoff value	AUC	Sensitivity (%)	Specificity (%)	Cutoff value
	ADC _{sc} *	0.97 ^a	94.1	94.9	1.5	0.97 ^{a,b}	94.1	94.4	1.5	—	—	—
Volume (cm ³)	0.86	77.3	88.1	237.1	0.71 ^a	77.3	66.7	237.1	—	—	—	—
ADC _{mean} *	—	—	—	—	—	—	—	—	0.79	76.2	76.2	2.0
10th percentile ADC*	—	—	—	—	0.72 ^b	77.3	76.2	1.5	0.72	85.7	52.4	1.2
50th percentile ADC*	0.72 ^a	77.3	69.1	2.2	—	—	—	—	0.81	61.9	95.2	2.4
90th percentile ADC*	0.81	68.2	88.1	2.5	—	—	—	—	0.85	73.8	90.5	2.6

AUC area under the curve

*, × 10⁻³ mm²/s

^{a, b}There was significant difference in AUC between the two parameters

0.71 and 0.72, $p = 0.003$ and 0.015 , respectively). For differentiating CCC from EC, the ADC_{mean} and 10th, 50th and 90th percentile ADCs had AUCs of 0.79, 0.72, 0.81 and 0.85, without significant differences in AUCs among the four histogram-derived parameters (all $p > 0.05$). To sum up all the significant results, a simple but clean diagnostic procedure for three types of tumors is displayed in Fig. 3.

Discussion

The present study demonstrated that the traditional ADC_{SC} had an excellent performance for differentiating between SMBT and CCC/EC, while the whole-tumor ADC histogram analysis had both complementary role and unique advantages for differentiating between CCC and EC.

There were no significant differences in clinical characteristics, such as age, tumor laterality and FIGO stage, between CCC and EC, similar to previous studies [10, 14]. Although it has been reported that SMBT can involve the bilateral ovaries in up to 40% of patients [5], in our study, all SMBT occurred in a unilateral ovary. The number of early-stage tumors and small sample size might explain the inconsistency. The mean age at diagnosis was significantly younger in patients with SMBT (39.91 ± 12.08 years) than in patients with CCC/EC ($51.48 \pm 9.52, 52.24 \pm 8.15$ years). This finding was consistent with a previous review that reported an average age of 34–44 years for patients with SMBT [6]. The volume of SMBT in our study (187.6 cm^3) was significantly smaller than that of CCC/EC ($537.0 \text{ cm}^3/280.1 \text{ cm}^3$). This finding is consistent with those of previous studies that showed a significantly smaller tumor size and a smaller portion of solid components in SMBT than in other endometriosis-related malignant tumors [1, 6]. In this study, most of the enrolled patients were at early FIGO stages (80.9% SMBTs, 97.6% CCCs and 100% ECs). Similar to the previous studies, of which up to 90% of SMBT patients presented as FIGO I stage, and CCC and EC patients were more likely to be diagnosed at early stages [5, 7]. Also, our results were consistent with the reported results of higher endometriosis coexisting in early disease [24, 25].

A previous study showed that SMBT had a higher ADC_{SC} value than CCC and EC [1]. This is generally understood as a consequence of greater tumor cellularity in malignancies, which limits the free diffusion of water molecules [26]. Our study also confirmed that the ADC_{SC} value was significantly higher in SMBT than in CCC and EC and yielded an excellent performance for differentiating SMBT from CCC and EC (both AUCs of 0.97). However, MRI findings of CCC and EC often overlap, and few studies have succeeded in differentiating them [10, 14, 27]. The morphological features of EC, such as multilocular cysts, a broad

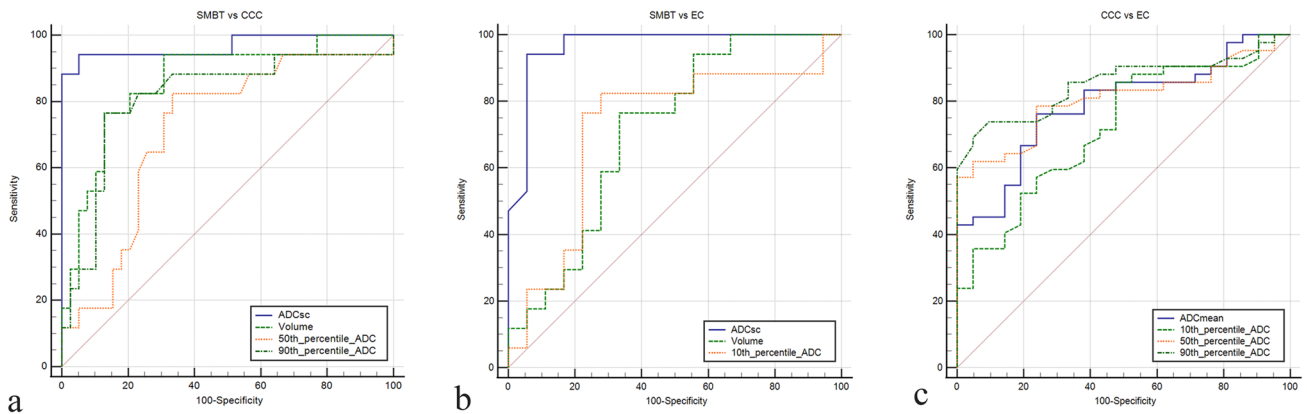


Fig. 2 ROC curves of the ADC_{SC} and whole-tumor histogram-derived parameters for the differentiation of SMBT, CCC and EC. **a** ROC curve for differentiating between SMBT and CCC. The AUCs of the ADC_{SC} , volume, and 50th and 90th percentile ADCs were 0.97, 0.86, 0.72 and 0.81, respectively, with no significant difference between the AUCs of the ADC_{SC} and volume ($p=0.097$) or the 90th percentile ADC ($p=0.053$), and with a significant difference between the AUCs of the ADC and 50th percentile ADC ($p=0.003$). **b** ROC

curve for differentiating between SMBT and EC. The AUC of the ADC_{SC} was 0.97, which was significantly higher than that of volume (0.71; $p=0.003$) and the 10th percentile ADC (0.72; $p=0.015$). **c** ROC curve for differentiating between CCC and EC. The AUCs of the ADC_{mean} and 10th, 50th and 90th percentile ADCs were 0.79, 0.72, 0.81 and 0.85, respectively, with no significant difference among them (all $p>0.05$). ADC_{SC} , ADC of solid components; *ROC* receiver operating characteristic; *AUC* area under the curve

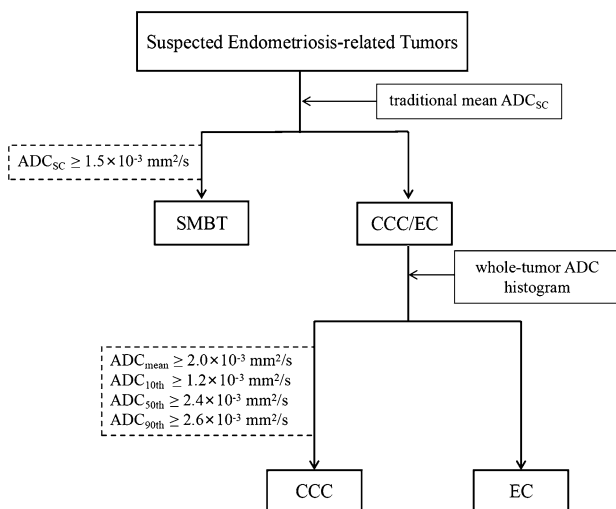


Fig. 3 Diagnostic procedure for differentiation of SMBT, CCC and EC. When endometriosis-related tumors are suspected clinically, traditional mean ADC_{sc} is firstly used. SMBT can be diagnosed excellently with $ADC_{sc} \geq 1.5 \times 10^{-3} \text{ mm}^2/\text{s}$. And then CCC and EC are discriminated with whole-tumor ADC histogram analysis. When ADC_{mean} and 10th, 50th and 90th percentile ADCs are more than 2.0, 1.2, 2.4 and $2.6 \times 10^{-3} \text{ mm}^2/\text{s}$, CCC can be diagnosed efficiently

base (small height/width ratio), a multifocal or continuing growth pattern of the mural nodules and the presence of ascites, were reported in different studies with AUCs ranging from 0.50 to 0.76 [10, 14]. One reported that the mean ADC_{SC} value was $1.24 \pm 0.17 \times 10^{-3} \text{ mm}^2/\text{s}$ in 17 cases of CCC, which was significantly higher than that of 14 cases of EC ($0.84 \pm 0.10 \times 10^{-3} \text{ mm}^2/\text{s}$) [15]. In our study, the ADC_{SC}

value was $1.2 \times 10^{-3} \text{ mm}^2/\text{s}$ in 42 cases of CCC, compared with $1.0 \times 10^{-3} \text{ mm}^2/\text{s}$ in 21 cases of EC, without a significant difference. Larger sample sizes and tumors with a histopathological confirmation of endometriosis might explain the difference between the two studies.

Although our whole-tumor histogram analysis showed no significant differences in the ADC_{mean} between the SMBT and CCC/EC groups, the 50th and 90th percentile ADCs were significantly lower in SMBT than in CCC, inconsistent with the ADC_{sc} . These findings could be explained by the different methods used to draw ROIs. In addition to the solid components of tumors, cystic contents were also included in the whole-tumor histogram analysis, which could compromise the ADC_{mean} differences between SMBT and CCC/EC. Whole-tumor ADC histogram analysis can provide more detailed information on the diffusion characteristics of tumors than traditional ADC values [15], allowing the evaluation of intratumoral heterogeneity [28]. No significant differences were found in inhomogeneity, entropy, skewness or kurtosis among SMBT, CCC and EC. ROI of whole-tumor components might be the reason. Endometriosis-related tumors usually present most of bloody cystic fluid and small part of solid components. The heterogeneity might be masked, and the differences among the three tumors might be compromised. The ADC_{mean} and 10th, 50th and 90th percentile ADCs could be useful for differentiating CCC from EC, and the 90th percentile ADC showed the largest AUC of 0.85. Previous studies have suggested that lower percentile ADCs might represent the hypercellular component of the tumor, while higher percentile ADCs might represent the cystic content of the tumor [18, 29, 30].

Our study showed a significantly lower 10th percentile ADC in EC than in SMBT and CCC, indicating greater tumor cellularity in EC, consistent with previous studies [1, 23, 26], and significantly higher 50th and 90th percentile ADCs in CCC than in SMBT and EC, indicating more cystic contents and smaller overall and solid portion sizes in SMBT and EC [1]. Furthermore, previous studies showed that the ADC value of the cystic content decreased as blood and protein concentrations increased [30], and the signal intensity of cystic contents on T1WI was significantly higher in SMBT than in CCC [5]. These findings could be ascribed either to hemorrhagic, mucinous and mucopurulent fluid in SMBT [5], or nonhemorrhagic serous fluid produced by the more malignant CCC [15] and different transformation pathways and time phases between CCC and EC [23, 31, 32].

Our study had several limitations. First, it was a retrospective study with a small sample size, especially the number of patients with SMBT. However, considering the rarity of SMBT, it might be difficult to perform a large cohort study. Second, some clinical information, such as the CA 125 level, was deficient in some cases, as we enrolled patients for a long period of time. A history of menstruation and related serum tests may provide additional information for the diagnosis of endometriosis-related diseases. Third, only ADC histogram analysis was performed in our study. Because endometriosis-related tumors undergo repeated cycles of hemorrhage, the different ages of the hemorrhage in the cysts tends to have a varied but characteristic signal on T1WI and T2WI. Histogram analysis of T1WI and T2WI may contribute to the differentiation of SMBT, CCC and EC.

Conclusions

In summary, this study demonstrated that the traditional ADC_{SC} had an excellent performance in differentiating SMBT from CCC/EC and was incompetent in differentiating CCC from EC, while the whole-tumor ADC histogram analysis had both complementary role in differentiate SMBT from CCC/EC, and unique advantages in differentiating CCC from EC.

Funding This work was supported by the National Natural Science Foundation of P.R. China [No. 81971579], Shanghai Municipal Commission of Science and Technology [No. 19411972000], Shanghai Municipal Health Commission [No. ZK2019B01] and Shanghai Jinshan District Health Commission [No.JSYQ201901].

Declarations

Conflict of interest The authors declare that they have no competing interests.

References

- Kurata Y, Kido A, Moribata Y, et al. Diagnostic performance of MR imaging findings and quantitative values in the differentiation of seromucinous borderline tumour from endometriosis-related malignant ovarian tumour. *Eur Radiol*. 2017, 27: 1695-1703.
- Maeda D, Shih I. Pathogenesis and the role of ARID1A mutation in endometriosis-related ovarian neoplasms. *Adv Anat Pathol*. 2013, 20: 45-52.
- Mary A W, Ie-Ming S, James H S, et al. cancer Implications for Patients with Endometriosis. *Semin Reprod Med*. 2017, 35: 110-116.
- Yoshikawa H, Jimbo H, Okada S et al. Prevalence of endometriosis in ovarian cancer. *Gynecol Obstet Invest*. 2000, 50 Suppl 1:11-7.
- Nagamine M, Mikami Y. Ovarian seromucinous tumors: pathogenesis, morphologic spectrum, and clinical issues. *Diagnostics (Basel)*. 2020, 10: 77.
- Karpathiou G, Chauleur C, Corsini T, et al. Seromucinous ovarian tumor a comparison with the rest of ovarian epithelial tumors. *Annals of Diagnostic Pathology*. 2017, 27: 28-33.
- NCCN Clinical practice guidelines in oncology: ovarian cancer including fallopian tube cancer and primary peritoneal cancer. Version 1.2021.
- Li HM, Feng F, Qiang JW, et al. Quantitative dynamic contrast-enhanced MR imaging for differentiating benign, borderline, and malignant ovarian tumors. *Abdom Radiol (NY)*. 2018, 43: 3132-3141.
- Guiu MX, Stewart CJR. Endometriosis-associated ovarian neoplasia. *Pathology*. 2018, 50: 190-204.
- Li M, Tan J, Zhang Y, et al. Assessing CT imaging features combined with CEA and CA125 levels to identify endometriosis-associated ovarian cancer. *Abdom Radiol (NY)*. 2021, 46: 2367-2375..
- Han J W, Kim K A, Chang H Y, et al. Newly categorized seromucinous tumor of the ovary: magnetic resonance imaging findings. *J Comput Assist Tomogr*. 2019, 43: 119-127.
- Kurata Y, Kido A, Moribata Y, et al. Differentiation of seromucinous borderline tumor from serous borderline tumor on MR imaging. *Magn Reson Med Sci*. 2018, 17: 211-217.
- Liu T, Sumida D, Wada T, et al. A diagnostic challenge of seromucinous borderline tumor: a case report. *Medicine (Baltimore)*. 2019, 98: e15707.
- Morioka S, Kawaguchi R, Yamada Y, et al. Magnetic resonance imaging findings for discriminating clear cell carcinoma and endometrioid carcinoma of the ovary. *J Ovarian Res*. 2019, 12: 20.
- Yumiko O T, Satoshi O, Takako Y, et al. MRI of endometriotic cysts in association with ovarian carcinoma. *AJR Am J Roentgenol*. 2010, 194: 355-361.
- Lu J, Li H M, Cai S Q, et al. Prediction of platinum-based chemotherapy response in advanced high-grade serous ovarian cancer: ADC histogram analysis of primary tumors. *Acad Radiol*. 2020: S1076-6332(20)30052-0.
- He M, Song Y, Li H, et al. Histogram analysis comparison of monoexponential, advanced diffusion-weighted imaging, and dynamic contrast-enhanced MRI for differentiating borderline from malignant epithelial ovarian tumors. *J Magn Reson Imaging*. 2020, 52: 257-268..
- Li H M, Zhang R, Gu W Y, et al. Whole solid tumour volume histogram analysis of the apparent diffusion coefficient for differentiating high-grade from low-grade serous ovarian carcinoma: correlation with Ki-67 proliferation status. *Clin Radiol*. 2019, 74: 918-925.
- Xu Y S, Liu H F, Xi D L, et al. Whole-lesion histogram analysis metrics of the apparent diffusion coefficient: a correlation study

- with histological grade of hepatocellular carcinoma. *Abdom Radiol (NY)*. 2019, 44: 3089-3098.
20. Xiao Z, Tang Z, Zhang J, et al. Whole-tumor histogram analysis of monoexponential and advanced diffusion-weighted imaging for sinonasal malignant tumors: Correlations with histopathologic features. *J Magn Reson Imaging*. 2020, 51: 273-285.
 21. Zhang Z, Song C, Zhang Y, et al. Apparent diffusion coefficient (ADC) histogram analysis: differentiation of benign from malignant parotid gland tumors using readout-segmented diffusion-weighted imaging. *Dentomaxillofac Radiol*. 2019, 48: 20190100.
 22. Pope W B, Kim H J, Huo J, et al. Recurrent glioblastoma multiforme: ADC histogram analysis predicts response to bevacizumab treatment. *Radiology*. 2009, 252: 182-189.
 23. Kyriazi S, Collins D J, Messiou C, et al. Metastatic ovarian and primary peritoneal cancer: assessing chemotherapy response with diffusion-weighted MR imaging--value of histogram analysis of apparent diffusion coefficients. *Radiology*. 2011, 261: 182-192.
 24. Zhou L, Yao L, Dai L, et al. Ovarian endometrioid carcinoma and clear cell carcinoma: A 21-year retrospective study. *J Ovarian Res*. 2021, 14:63.
 25. Kim H S, Kim T H, Chung H H, et al. Risk and prognosis of ovarian cancer in women with endometriosis: a meta-analysis. *Br J Cancer*. 2014, 110:1878-1890.
 26. Zhang Y D, Wu C J, Wang Q, et al. Comparison of utility of histogram apparent diffusion coefficient and R2* for differentiation of low-grade from high-grade clear cell renal cell carcinoma. *AJR Am J Roentgenol*. 2015, 205: W193-W201.
 27. Ono T, Kishimoto K, Tajima S, et al. Apparent diffusion coefficient (ADC) values of serous, endometrioid, and clear cell carcinoma of the ovary: pathological correlation. *Acta Radiol*. 2020, 61: 992-1000.
 28. Schob S, Meyer H, Dieckow J, et al. Histogram analysis of diffusion weighted imaging at 3T is useful for prediction of lymphatic metastatic spread, proliferative activity, and cellularity in thyroid cancer. *Int J Mol Sci*. 2017, 18: 821.
 29. Wang F, Wang Y X, Zhou Y, et al. Apparent diffusion coefficient histogram analysis for assessing tumor staging and detection of lymph node metastasis in epithelial ovarian cancer: correlation with p53 and Ki-67 expression. *Mol Imaging Biol*. 2019, 21: 731-739.
 30. Moteki T, Horikoshi H, Endo K. Relationship between apparent diffusion coefficient and signal intensity in endometrial and other pelvic cysts. *Magn Reson Imaging*. 2002, 20: 463-470.
 31. Kato N, Sasou S, Motoyama T. Expression of hepatocyte nuclear factor-1beta (HNF-1beta) in clear cell tumors and endometriosis of the ovary. *Mod Pathol*. 2006, 19: 83-89.
 32. Xiao W B, Awadallah A, Xin W. Loss of ARID1A/BAF250a expression in ovarian endometriosis and clear cell carcinoma. *Int J Clin Exp Pathol*. 2012, 5: 642-650.

Publisher's Note Springer Nature remains neutral with regard to jurisdictional claims in published maps and institutional affiliations.

Springer Nature or its licensor (e.g. a society or other partner) holds exclusive rights to this article under a publishing agreement with the author(s) or other rightsholder(s); author self-archiving of the accepted manuscript version of this article is solely governed by the terms of such publishing agreement and applicable law.